JCI The Journal of Clinical Investigation

Distinct mechanisms of TGF-β1–mediated epithelial-to-mesenchymal transition and metastasis during skin carcinogenesis

Gangwen Han, … , Molly Kulesz-Martin, Xiao-Jing Wang

J Clin Invest. 2005;115(7):1714-1723. https://doi.org/10.1172/JCI24399.

Research Article **Oncology**

In the present study, we demonstrated that human skin cancers frequently overexpress TGF-β but exhibit decreased expression of the TGF-β type II receptor (TGF-βRII). To understand how this combination affects cancer prognosis, we generated a transgenic mouse model that allowed inducible expression of TGF-β_1 in keratinocytes expressing a dominant negative TGF-βRII (ΔβRII) in the epidermis. Without ΔβRII expression, TGF-β_1 transgene induction in late-stage, chemically induced papillomas failed to inhibit tumor growth but increased metastasis and epithelial-to-mesenchymal transition (EMT), i.e., formation of spindle cell carcinomas. Interestingly, ΔβRII expression abrogated TGF-β_1–mediated EMT and was accompanied by restoration of membrane-associated E-cadherin/catenin complex in TGF-β_1/ΔβRII compound tumors. Furthermore, expression of molecules thought to mediate TGF-β_1–induced EMT was attenuated in TGF-β_1/ΔβRII–transgenic tumors. However, TGF-β_1/ΔβRII–transgenic tumors progressed to metastasis without losing expression of the membrane-associated E-cadherin/catenin complex and at a rate higher than those observed in nontransgenic, TGF-β_1–transgenic, or ΔβRII-transgenic mice. Abrogation of Smad activation by ΔβRII correlated with the blockade of EMT. However, ΔβRII did not alter TGF-β_1–mediated expression of RhoA/Rac and MAPK, which contributed to increased metastasis. Our study provides evidence that TGF-β_1 induces EMT and invasion via distinct mechanisms. TGF-β_1–mediated EMT requires functional TGF-βRII, whereas TGF-β_1–mediated tumor invasion cooperates with reduced TGF-βRII signaling in tumor epithelia.

Distinct mechanisms of TGF-β_1–mediated epithelial-to-mesenchymal transition and metastasis during skin carcinogenesis

Gangwen Han,[1] Shi-Long Lu,[1] Allen G. Li,[1,2] Wei He,[3] Christopher L. Corless,[4] Molly Kulesz-Martin,[2,5] and Xiao-Jing Wang[1,2,5]

[1]Department of Otolaryngology and [2]Department of Dermatology, Oregon Health & Science University, Portland, Oregon, USA. [3]Xinqao Hospital, Chongqing, China. [4]Department of Pathology and [5]Department of Cell and Developmental Biology, Oregon Health & Science University, Portland, Oregon, USA.

In the present study, we demonstrated that human skin cancers frequently overexpress TGF-β_1 but exhibit decreased expression of the TGF-β type II receptor (TGF-βRII). To understand how this combination affects cancer prognosis, we generated a transgenic mouse model that allowed inducible expression of TGF-β_1 in keratinocytes expressing a dominant negative TGF-βRII (ΔβRII) in the epidermis. Without ΔβRII expression, TGF-β_1 transgene induction in late-stage, chemically induced papillomas failed to inhibit tumor growth but increased metastasis and epithelial-to-mesenchymal transition (EMT), i.e., formation of spindle cell carcinomas. Interestingly, ΔβRII expression abrogated TGF-β_1–mediated EMT and was accompanied by restoration of membrane-associated E-cadherin/catenin complex in TGF-β_1/ΔβRII compound tumors. Furthermore, expression of molecules thought to mediate TGF-β_1–induced EMT was attenuated in TGF-β_1/ΔβRII–transgenic tumors. However, TGF-β_1/ΔβRII–transgenic tumors progressed to metastasis without losing expression of the membrane-associated E-cadherin/catenin complex and at a rate higher than those observed in nontransgenic, TGF-β_1–transgenic, or ΔβRII-transgenic mice. Abrogation of Smad activation by ΔβRII correlated with the blockade of EMT. However, ΔβRII did not alter TGF-β_1–mediated expression of RhoA/Rac and MAPK, which contributed to increased metastasis. Our study provides evidence that TGF-β_1 induces EMT and invasion via distinct mechanisms. TGF-β_1–mediated EMT requires functional TGF-βRII, whereas TGF-β_1–mediated tumor invasion cooperates with reduced TGF-βRII signaling in tumor epithelia.

Introduction

TGF-β_1 is a potent growth inhibitor for epithelial cells, and this function contributes greatly to its role in tumor suppression (1). Paradoxically, TGF-β_1 is overexpressed in many malignant human tumors including squamous cell carcinomas (SCCs) (2–4) and in various cancers in experimental animals, including skin tumors (for review, see ref. 5). Studies have shown that TGF-β_1 overexpression at early stages of carcinogenesis provides tumor-suppressive effects primarily via growth inhibition (1), whereas TGF-β_1 overexpression at late stages promotes tumor progression, metastasis, and epithelial-to-mesenchymal transition (EMT), potentially via loss of adhesion molecules, angiogenesis, proteinase activation, and immune suppression (1, 6).

TGF-β_1 exerts its effects primarily via a receptor complex comprising a type I and a type II receptor (TGF-βRI and TGF-βRII). To date, only 1 TGF-βRII has been identified that is essential for TGF-β binding and for assembly of the TGF-βRI/TGF-βRII complex (7). When TGF-β binds to a TGF-βRI/TGF-βRII complex, TGF-βRI phosphorylates Smad2 and Smad3. Phosphorylated Smad2 (pSmad2) and pSmad3 form heteromeric complexes with Smad4 and translocate into the nucleus to regulate TGF-β–responsive genes (7). Several Smad-independent TGF-β signaling pathways have also been identified, including the RhoA and MAPK pathways (7). Whereas TGF-β_1 is overexpressed in cancer cells, TGF-βRII is often lost in cancer cells (1). It is commonly accepted that the tumor-suppressive effect of TGF-β_1 requires functional TGF-βRII; therefore, inactivation of TGF-βRII is an important mechanism by which tumor cells escape TGF-β_1–mediated growth inhibition and progress to malignancy. However, with respect to the role of TGF-βRII in TGF-β_1–mediated tumor promotion, the data are controversial. In vitro studies have shown that TGF-βRII is required for TGF-β_1–mediated tumor invasion (8, 9). Decreased breast cancer metastasis was seen in a model expressing a dominant negative TGF-βRII (ΔβRII) transgene in human breast-derived cell lines (10). In contrast, increased skin cancer metastasis and prostate cancer metastasis were observed in the respective ΔβRII-transgenic models (11, 12). Clinical studies also reveal controversial results regarding patient outcome when the prognosis is correlated with the loss of TGF-βRII in cancer cells. For instance, loss of TGF-βRII expression correlates with poor prognosis in esophageal cancer (13) and renal carcinoma (14) but correlates with a better survival rate in colon cancer (15) and gastric cancer (16). These observations highlight the complex nature of the functions of TGF-βRII in carcinogenesis, which could be stage and/or tissue specific. Although TGF-β_1 overexpression and loss of TGF-βRII have been observed in human HaCaT keratinocytes with oncogenic potential (17, 18), whether these changes occur in primary SCCs in the skin has not been reported.

The mouse skin chemical carcinogenesis model is a useful tool for studying different stages of carcinogenesis. This model mimics the multistage nature of cancer development in humans, i.e.,

Nonstandard abbreviations used: ΔβRII, dominant-negative TGF-βRII; AK, actinic keratosis; CIS, carcinoma in situ; DMBA, dimethylbenzanthracene; EMT, epithelial-to-mesenchymal transition; Jag1, Jagged 1; K14, keratin 14; *ML*, *mouse loricrin* promoter; pSmad2, phosphorylated Smad2; RPA, RNase protection assay; SCC, squamous cell carcinoma; SPCC, spindle cell carcinoma; TGF-βRII, TGF-β type II receptor; *tk*, *thymidine kinase* promoter; TPA, 12-*O*-tetradecanoylphorbol-13-acetate.

Conflict of interest: The authors have declared that no conflict of interest exists.

Citation for this article: *J. Clin. Invest.* **115**:1714–1723 (2005). doi:10.1172/JCI24399.

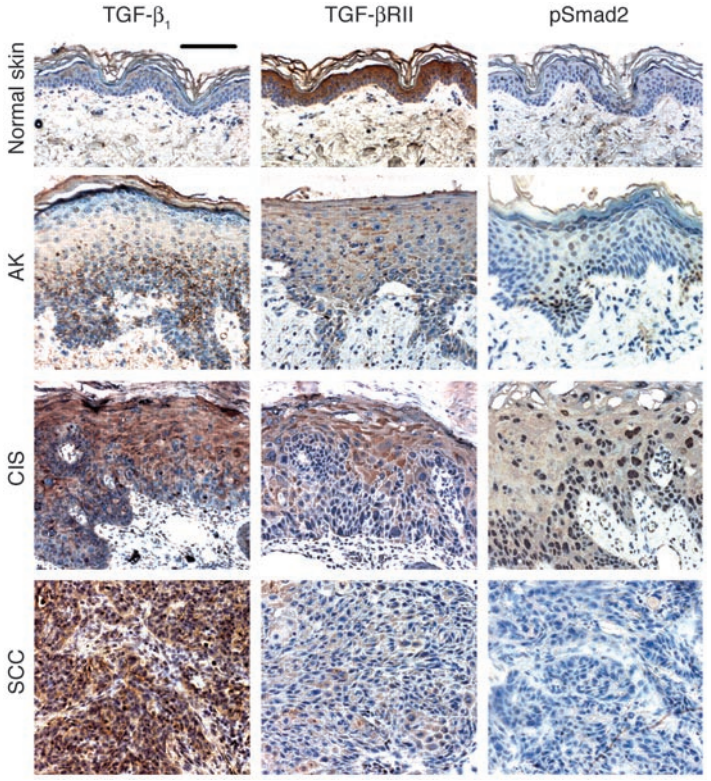

Figure 1
Immunostaining for TGF-β_1, TGF-βRII, and pSmad2 in human skin cancer samples revealed a patchy increase in TGF-β_1 and decrease in TGF-βRII staining in AK and CIS, and the same alterations were uniform in SCC. pSmad2-positive cells were detected in AK and CIS. Scale bar: 40 μm for all panels.

initiation, promotion, and malignant conversion (19). Initiation is induced by topical application of a subcarcinogenic dose of a particular carcinogen, e.g., dimethylbenzanthracene (DMBA). Following initiation, a tumor promoter, e.g., 12-*O*-tetradecanoylphorbol-13-acetate (TPA), is applied to elicit benign papillomas. After promotion, papillomas can persist, regress, or convert to malignancy (19). In this experimental model, expression of endogenous TGF-β_1 is induced by TPA at a very early stage and persists in malignant carcinomas (5), and loss of endogenous TGF-βRII protein occurs at the stage of carcinoma formation (6). When this 2-stage carcinogenesis protocol was applied to transgenic mice overexpressing TGF-β_1 in the epidermis, TGF-β_1 transgene expression inhibited benign tumor formation yet enhanced progression to carcinomas (6, 20). Since TGF-β_1 transgene expression began at a relatively early stage in both studies, it remains to be determined whether the tumor promotion effect is the result of long-term TGF-β_1 overexpression, which creates a selective advantage for TGF-β_1–resistant tumors, or whether late-stage tumors by their own nature can escape TGF-β_1–mediated growth inhibition. In either case, it is not clear whether functional TGF-βRII is required for TGF-β_1–mediated tumor promotion. In contrast to in vitro studies showing that TGF-β receptors are required for TGF-β_1–mediated tumor invasion (8, 9, 21, 22), our previous results have shown that TGF-β_1–transgenic tumors exhibited earlier loss of TGF-βRII and signaling Smads (6). These results suggest that downregulation of specific TGF-β signaling components in tumor epithelia selectively abolishes TGF-β_1–mediated growth inhibition but may not affect all of the tumor-promoting activities of TGF-β_1.

In the present study, we found that human skin cancers often overexpress TGF-β_1 but exhibit decreased expression of TGF-βRII. To further investigate how this combination affects cancer progression, we bred ΔβRII mice with gene-switch–TGF-β_1 mice in which TGF-β_1 transgene expression can be induced in ΔβRII tumor epithelia at specific stages of skin carcinogenesis (23). We provide in vivo evidence that loss of functional TGF-βRII in tumor epithelia selectively blocks the molecular and pathological alterations required for TGF-β_1–mediated EMT but cooperates with TGF-β_1 for tumor invasion.

Results

Altered expression of TGF-β_1 signaling components in human skin cancer. To determine whether expression of TGF-β signaling components is altered in human skin cancer, we performed immunostaining for TGF-β_1, TGF-βRII, and nuclear pSmad2, a marker for activation of TGF-β signaling (7). Among the tissue samples examined were 8 normal skin, 14 actinic keratoses (AKs), 9 carcinomas in situ (CISs), and 34 SCCs. In normal skin, TGF-β_1 exhibited weak staining in the epidermis and dermis (Figure 1). TGF-βRII exhibited staining at the highest intensity in normal epidermis compared with the other tissue samples examined (Figure 1). As shown in Table 1, in the progression from AK to CIS to SCC, there was a clear overall trend toward increased TGF-β_1 and decreased TGF-βRII expression. The combination of both increased TGF-β_1 and reduced TGF-βRII was detected at a rate of 7% in AK, 22% in CIS, and 38% in SCCs, with expression in normal epidermis serving as a baseline (Table 1). The increase in TGF-β_1 staining appeared patchy in AKs and gradually became uniform when progressing to CISs and SCCs (Figure 1). The decrease in TGF-βRII staining appeared uniform or patchy in AKs and CISs (Figure 1), but the reduction was generally uniform in SCCs (Figure 1). Nuclear staining of pSmad2 was not detected in normal skin (Figure 1), which suggests that the baseline level of TGF-β signaling via the Smad pathway is very low. Nuclear staining for pSmad2 was detectable in 3 AK samples and 4 CIS samples, all of which exhibited both increased TGF-β_1 staining intensity and the presence of TGF-βRII (Figure 1). Staining of pSmad2 was not detected in 32 of 34 SCC samples (94%; Table 1) regardless of the levels of TGF-β_1 expression (Figure 1).

Table 1
Expression of TGF-β_1, TGF-βRII, and pSmad2 in human skin cancer samples as detected by immunostaining

Sample type (total no.)	No. of samples with			
	TGF-β_1↑	TGF-βRII↓	TGF-β_1↑ and TGF-βRII↓	Nuclear pSmad2
Normal skin (8)	0 (0%)	0 (0%)	0 (0%)	0 (0%)
AK (14)	3 (21%)	5 (36%)	1 (7%)	3 (21%)
CIS (9)	4 (44%)[A]	4 (44%)[A]	2 (22%)	4 (44%)[A]
SCC (34)	18 (53%)[A,B]	19 (56%)[A,B]	13 (38%)[A,B]	2 (6%)[C]

The χ^2 test ($P < 0.05$) was used for comparisons with [A]normal skin, [B]AK, or [C]CIS. All samples with nuclear pSmad2 exhibited increased TGF-β_1 and retained TGF-βRII. ↑, increase; ↓, decrease.

Table 2
Genotypes and numbers of mice used in the chemical carcinogenesis experiment

Group (total no.)	Genotype (no.)	Sex	
		M	F
Control (44)	Nontransgenic (14)	8	6
	ML.GLVPc (13)	6	7
	tk.TGF-β1 (8)	4	4
	ML.GLVPc/tk.TGF-β1 treated with ethanol solvent (9)	5	4
	Total no.	23	21
TGF-β1 (20)	*ML.GLVPc/tk.TGF-β1* (20)	11	9
ΔβRII (27)	*ML.ΔβRII* (15)	7	8
	tk.TGF-β1/ML.ΔβRII (12)	7	5
	Total no.	14	13
TGF-β1/ΔβRII (15)	*ML.GLVPc/tk.TGF-β1/ML.ΔβRII* (15)	7	8

All mice were treated with the same regimen of RU486 starting at 20 weeks after DMBA initiation, except as otherwise indicated in the table.

Tumor progression in gene-switch–TGF-β1 and TGF-β1/ΔβRII–transgenic tumors. Gene-switch–TGF-β1 mice (designated hereafter as TGF-β1–transgenic mice), in which epidermal TGF-β1 expression can be specifically regulated, and mice expressing ΔβRII in the epidermis (ΔβRII-transgenic mice) were generated in the ICR strain as described previously (23, 24). As we have previously reported, ΔβRII-transgenic neonates exhibit hyperproliferative epidermis due to blocked TGF-β1–induced growth inhibition but normalizes in adulthood (24), whereas gene-switch–TGF-β1 skin is normal prior to TGF-β1 transgene induction by RU486 but undergoes epidermal growth inhibition upon TGF-β1 induction (23). These mice were crossbred to generate TGF-β1/ΔβRII–transgenic mice, in which TGF-β1 transgene expression can be induced in tumor epithelia with constitutive ΔβRII expression. As shown in Table 2, littermates were divided into different groups based on genotypes and exposed to the 2-stage skin chemical carcinogenesis protocol, which is outlined in Figure 2A. TGF-β1 transgene expression was induced by topical application of a progesterone antagonist, RU486 (20 μg/mouse, 3 times/week) to bigenic mouse skin, beginning at 20 weeks after DMBA initiation (Figure 2A). As previously documented (25), the dose of RU486 used in this study is at least 1,000-fold lower than that required to exert any antagonistic effect on endogenous steroid receptors and does not affect the tumor kinetics or tumor types when this skin chemical carcinogenesis protocol is used on male or female mice. Nevertheless, we included RU486-treated nontransgenic and monogenic mice as controls (Table 2). Once lesions developed that appeared to be SCCs (ulcerated lesions), tumor-bearing mice were euthanized. All tumors on each euthanized mouse were excised and preserved for analyses. After all visible skin tumors were excised, necropsy was performed on each mouse to identify potential metastatic lesions. Tumor types (primary and metastatic lesions) were confirmed by histological analysis. The experiment was terminated by 40 weeks because the majority of transgenic mice had been euthanized due to development of aggressive skin tumors.

Among control mice with different genotypes (Table 2), we did not observe a difference in tumor kinetics. Therefore, tumor kinetics data among these mice were pooled. For the same reason, tumor kinetics data among different genotypes representing ΔβRII transgenics (Table 2) were also pooled. Prior to RU486 application (i.e., prior to induction of TGF-β1), tumor kinetics in TGF-β1–transgenic mice was essentially the same as that in control mice (Figure 2B) and was also similar to that in nontransgenic mice without RU486 treatment as we reported previously (6, 11). In contrast, TGF-β1/ΔβRII–transgenic mice exhibited earlier tumor formation and a 2- to 3-fold increase in tumor number compared with control mice ($P < 0.01$; Figure 2B). The tumor kinetics of TGF-β1/ΔβRII–transgenic mice was essentially the same as that of ΔβRII-transgenic mice (Figure 2B). After withdrawal of TPA promotion, the tumor kinetics in each group did not significantly change, despite the fact that regression appeared to be more noticed in control and ΔβRII-transgenic mice than in TGF-β1–transgenic or TGF-β1/ΔβRII–transgenic mice ($P > 0.05$). However, malignant conversion rates varied significantly among these groups. By 25 weeks after DMBA initiation, i.e., 5 weeks with TGF-β1 transgene induction, 73% of the TGF-β1/ΔβRII–transgenic mice developed SCCs (Table 3). Similar to the findings in our previous reports (6, 11), at 25 weeks, none of the control mice had developed SCCs, and 20% of the TGF-β1–transgenic mice and 11% of the ΔβRII-transgenic mice

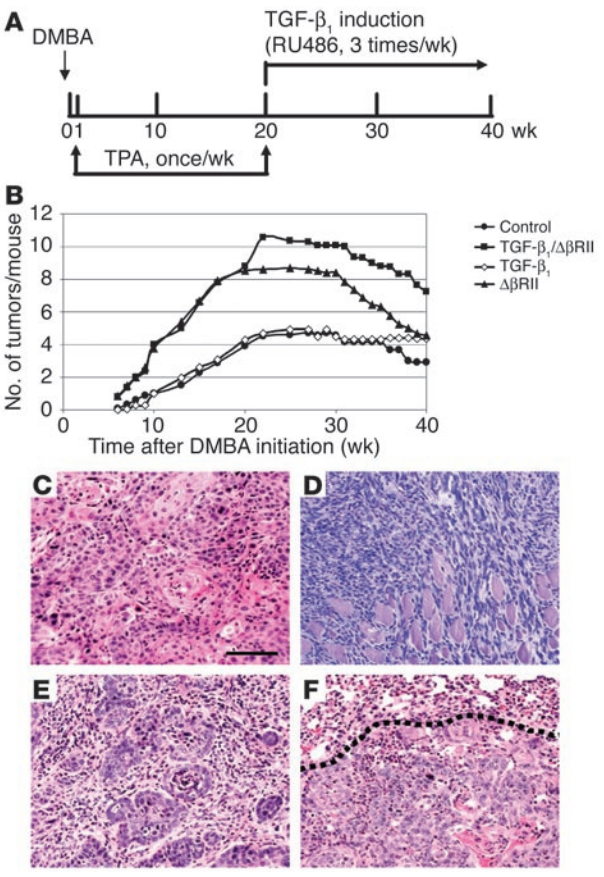

Figure 2
Skin tumor formation and tumor types in transgenic mice. (**A**) Schematic of the skin chemical carcinogenesis and TGF-β1 transgene induction protocol. (**B**) Kinetics of tumor formation. Each point represents the average number of tumors per mouse. (**C**) H&E staining of TGF-β1/ΔβRII–transgenic SCC. (**D**) TGF-β1–transgenic SPCC. (**E**) Metastatic lesion in lymph node showing SCC cells surrounded by lymphocytes. (**F**) Lung metastasis that originated from TGF-β1/ΔβRII–transgenic SCCs. The dotted line delineates lung tissue adjacent to the metastatic lesion. Scale bar in **C**: 40 μm for **C**–**F**.

Table 3
Rates of malignant conversion and metastasis in mice with different genotypes

Genotype (total no. of mice)	No. of mice with malignant tumors			No. of mice with metastasis	
	25 wk	30 wk	40 wk	30 wk	40 wk
Control (44)	0 (0%)	8 (18%)	10 (23%)	0 (0%)	1 (2%)
Δβ*RII* (27)	3 (11%)	6 (22%)	21 (78%)^{A}	3 (11%)^{A}	7 (26%)^{A}
TGF-β1 (20)	4 (20%)^{A,B}	10 (50%)^{A,B}	13 (65%)^{A}	2 (10%)^{A}	5 (25%)^{A}
TGF-β1/Δβ*RII* (15)	11 (73%)^{A,B,C}	12 (80%)^{A,B,C}	12 (80%)^{A}	3 (20%)^{A}	9 (60%)^{A,B,C}

The χ^2 test ($P < 0.05$) was used for comparisons with ^{A}control, ^{B}ΔβRII, or ^{C}TGF-β_1 within each column.

had developed SCCs (Table 3). At other time points throughout the entire course of the carcinogenesis experiment, TGF-β_1/ΔβRII–transgenic mice had the highest malignant conversion rate, followed by TGF-β_1–transgenic mice, then ΔβRII-transgenic mice (Table 3). In contrast, papillomas in control mice progressed to SCCs very slowly, which is typically observed in experiments using this carcinogenesis protocol (6, 11), having the lowest rate at all time points compared with any transgenic group in this study (Table 3). Almost all of the TGF-β_1/ΔβRII–transgenic tumors were classified as SCCs, ranging from well to poorly differentiated (Figure 2C). Approximately 30% of the TGF-β_1–transgenic mice developed spindle cell carcinoma (SPCC; Figure 2D), a typical EMT tumor type. SPCC cells generally constituted the entire lesion (Figure 2D), but in some cases, they were adjacent to SCC cells (data not shown). SPCC formation rarely occurred in ΔβRII-transgenic, TGF-β_1/ΔβRII–transgenic, or control mice. Furthermore, TGF-β_1– or ΔβRII-transgenic tumors metastasized to lymph nodes beginning 30 weeks after DMBA initiation, and by 40 weeks, both groups of mice developed metastatic lesions at a similar rate (~25%; Table 3). TGF-β_1/ΔβRII–transgenic mice also began to develop metastatic lesions at around 30 weeks. By 40 weeks, 60% of the TGF-β_1/ΔβRII–transgenic mice developed metastatic lesions in lymph nodes and/or lungs (Figure 2, E and F). All of the metastatic lesions in TGF-β_1/ΔβRII–transgenic mice were SCCs but not SPCCs. In contrast, only 1 control mouse developed metastasis by 40 weeks after DMBA initiation (Table 3).

TGF-β1 expression levels in tumors with different genotypes. We have previously shown that both TGF-β_1– and ΔβRII-transgenic mice exhibited increased malignant conversion and metastasis (6, 11); the latter correlated with increased endogenous TGF-β_1 expression (11). To determine whether the kinetics of malignant conversion and metastasis observed in this study correlated with TGF-β_1 levels, we examined TGF-β_1 expression levels in SCCs 25 weeks after DMBA initiation. The porcine TGF-β_1–transgenic transcripts were detected only in TGF-β_1– or TGF-β_1/ΔβRII–transgenic SCCs (Figure 3A). Analysis of total levels of TGF-β_1 protein in these tumor samples revealed that chemically induced SCCs in control mice exhibited an approximately 3-fold increase in endogenous TGF-β_1 protein compared with normal skin (169.6 ± 17.7 pg/mg protein vs. 53.6 ± 13.3 pg/mg protein; $n = 5$; $P < 0.01$; Figure 3B). Similar to what we have previously observed, ΔβRII-transgenic SCCs exhibited further elevation in endogenous TGF-β_1 protein level (233.3 ± 42.9 pg/mg protein; $n = 5$; $P < 0.05$ compared with control SCCs). TGF-β_1 protein levels were the highest in TGF-β_1–transgenic SCCs (374.7 ± 83.5 pg/mg protein; $n = 5$; $P < 0.01$ compared with ΔβRII-transgenic tumors), and TGF-β_1/ΔβRII–transgenic tumors exhibited TGF-β_1 protein levels similar to those in TGF-β_1–transgenic tumors (341.5 ± 109.4 pg/mg protein; $n = 5$). Notably, the variations in TGF-β_1 protein levels among these groups were very similar to those in human head and neck SCCs, as we have previously reported (4).

Late-stage papillomas escaped TGF-β1–mediated growth arrest. The tumor kinetics of the TGF-β_1–transgenic tumors suggests that after a full course of TPA promotion, papillomas developed the ability to escape TGF-β_1–mediated tumor suppression. To determine whether tumors at this stage have lost TGF-β_1–mediated growth inhibition or whether tumor cells still respond to TGF-β_1–mediated growth inhibition but only clonal TGF-β_1–resistant cells further progress to malignancy, we performed in vivo BrdU labeling on expressing and control tumors at 21 weeks (i.e., after the first 3 RU486 treatments). As expected, TGF-β_1–transgenic epidermis adjacent to tumors (Figure 4B) exhibited a lesser degree of hyperplasia compared with control epidermis adjacent to tumors (Figure 4A). The BrdU labeling index was 50 ± 3 cells/mm epidermis in TGF-β_1–transgenic epidermis adjacent to tumors ($n = 5$; Figure 4B), a nearly 3-fold reduction compared with that in control epidermis adjacent to tumors (143 ± 5 cells/mm epidermis; $n = 5$; $P < 0.01$; Figure 4A). The BrdU-labeling index in TGF-β_1–transgenic papillomas (176 ± 18.2 nuclei/mm^2 tumor epithelia; $n = 5$; Figure 4D) was similar to that of control papillomas (157 ± 16.1 nuclei/mm^2 tumor epithelia; $n = 5$; $P > 0.05$; Figure 4C). These results suggest that chemically induced papillomas at this stage no longer respond to TGF-β_1–mediated growth inhibition.

To determine whether the resistance to TGF-β_1–mediated growth inhibition in late-stage TGF-β_1–transgenic papillomas was due to the loss of TGF-β signaling at this stage, we performed

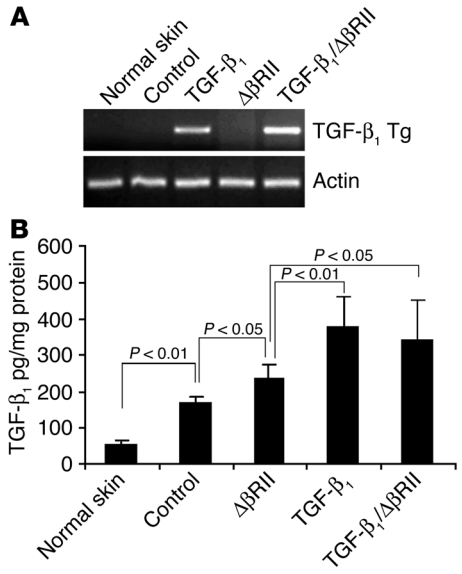

Figure 3
TGF-β_1 expression levels in mouse tumors with different genotypes. (**A**) Results of RT-PCR for TGF-β_1 transgene expression in TGF-β_1– and TGF-β_1/ΔβRII–transgenic SCCs. (**B**) Results of TGF-β_1–specific ELISA. Each group contained 4–6 samples.

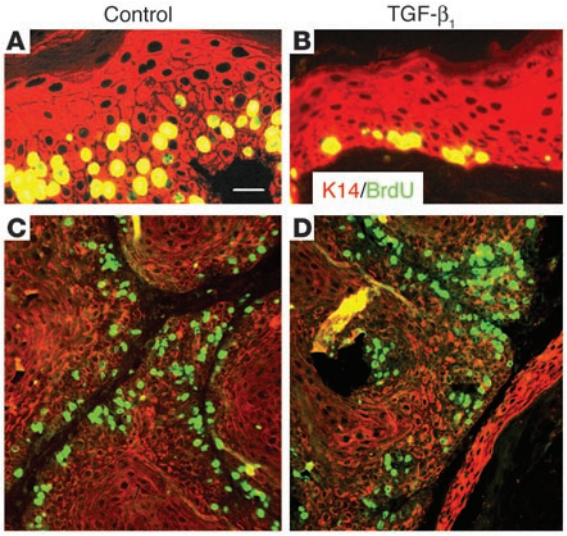

Figure 4
BrdU labeling in skin and papillomas 21 weeks after DMBA initiation and 1 week with (TGF-β_1) or without (Control) TGF-β_1 transgene induction. (**A**) Control skin adjacent to a papilloma. (**B**) TGF-β_1–transgenic skin adjacent to a papilloma. (**C**) Control papilloma. (**D**) TGF-β_1–transgenic papilloma. Scale bar in **A**: 20 μm for **A** and **B**; 40 μm for **C** and **D**.

immunohistochemical staining for pSmad2. In control papillomas, approximately 30% of the papilloma cells exhibited nuclear pSmad2 staining (Figure 5). This is likely due to elevated endogenous TGF-β signaling during skin carcinogenesis (11), as nuclear staining of pSmad2 was almost completely absent in ΔβRII-transgenic papillomas at the same stage (Figure 5). However, after 3 RU486 treatments, TGF-β_1–transgenic papillomas exhibited a further increase in pSmad2 staining, i.e., approximately 90% of the cells exhibited nuclear pSmad2 staining (Figure 5). This suggests that the ability of these tumor cells to escape from TGF-β_1–mediated growth arrest is not due to abrogation of TGF-β signaling. Nuclear staining of pSmad2 was absent in TGF-β_1/ΔβRII–transgenic papillomas (Figure 5), which indicates that ΔβRII expression blocked TGF-β_1–mediated Smad activation. Staining of pSmad2 in SCCs of TGF-β_1–transgenic mice after 5 weeks of TGF-β_1 transgene expression was negative in the nucleus and very weak in the cytoplasm (Figure 5). The SCCs from control, ΔβRII-, and TFGβ_1/ΔβRII–transgenic mice failed to exhibit any staining for pSmad2 (Figure 5), which is consistent with our previous report that Smad proteins are lost in SCCs during skin chemical carcinogenesis (26).

TGF-β_1 transgene induction in tumor epithelia resulted in earlier loss of membrane-associated E-cadherin/catenin complexes, an effect that was blocked by ΔβRII expression. Previously, we have observed that TGF-β_1 transgene induction resulted in earlier loss of membrane-associated E-cadherin/catenin complexes (6). To determine whether loss of E-cadherin/catenin complexes is associated with EMT and/or metastasis, we examined expression of E-cadherin, β-catenin, and γ-catenin in ΔβRII-, TGF-β_1–, and TGF-β_1/ΔβRII–transgenic tumors. Similar to nonexpressing tumors, ΔβRII-transgenic SCCs at 25 weeks after DMBA initiation retained membrane-associated E-cadherin and β- and γ-catenins (Figure 6). In contrast, TGF-β_1–transgenic SCCs at the same stage had lost membrane-associated E-cadherin and β- and γ-catenins, which were detected in the cytoplasm (Figure 6). Western blot analysis revealed no significant differences in the levels of these proteins between control and TGF-β_1–transgenic tumors (data not shown), which suggests that loss of membrane-associated forms of these molecules was due to redistribution to the cytoplasm. Interestingly, localization of E-cadherin and β- and γ-catenins in TGF-β_1/ΔβRII–transgenic tumors was similar to that in ΔβRII-transgenic tumors (Figure 6), which indicates that expression of ΔβRII was able to abrogate TGF-β_1–mediated redistribution of the E-cadherin/catenin complex. Membrane-associated E-cadherin/catenins were eventually lost in some of the late-stage ΔβRII-transgenic SCCs or TGF-β_1/ΔβRII–transgenic SCCs at approximately the same stage as when these changes occurred in control SCCs (data not shown). Similar to cells from primary tumors of each genotype, metastatic tumor cells that developed from TGF-β_1–transgenic tumors exhibited cytoplasmic staining of the above-mentioned adhesion molecules (data not shown). In contrast, metastatic cells that originated from ΔβRII-transgenic SCCs (data not shown) or TGF-β_1/ΔβRII–transgenic SCCs (Figure 6) still exhibited membrane-associated cell adhesion molecules, which suggests that metastasis in these tumors occurred without or prior to the loss of membrane-associated E-cadherin/catenins.

TGF-β_1/ΔβRII–transgenic SCCs exhibited the most severe angiogenesis. Since TGF-β_1/ΔβRII–transgenic tumors exhibited the highest rate of metastasis, we suspected that ΔβRII expression may not block the effects of TGF-β_1 on pathological alterations related to invasion. Therefore, we examined angiogenesis. Immunofluorescence staining using a CD31 antibody on SCCs 25 weeks after DMBA initiation revealed that the percentage of stromal area covered by vessels was 36.5% ± 4.9% in control SCCs, 56.9% ± 9.1% in TGF-β_1–transgenic SCCs, and 59% ± 6.9% in ΔβRII-transgenic SCCs (Figure 7, A and B). TGF-β_1/ΔβRII–transgenic SCCs exhibited the greatest amount of vessels covering the stromal area (70.1% ± 9.3%; Figure 7, A and B). We also examined these tumors for expression levels of VEGF and its receptor VEGFR1. VEGF was expressed at comparable

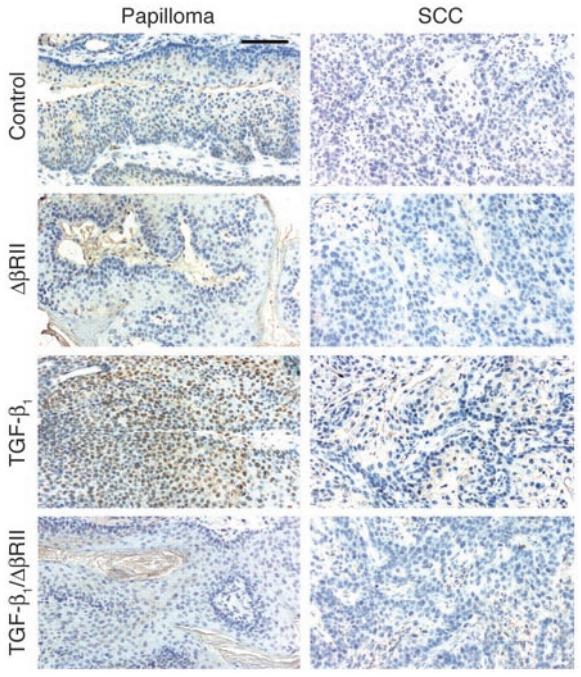

Figure 5
Immunohistochemistry for pSmad2. Scale bar: 40 μm for all panels.

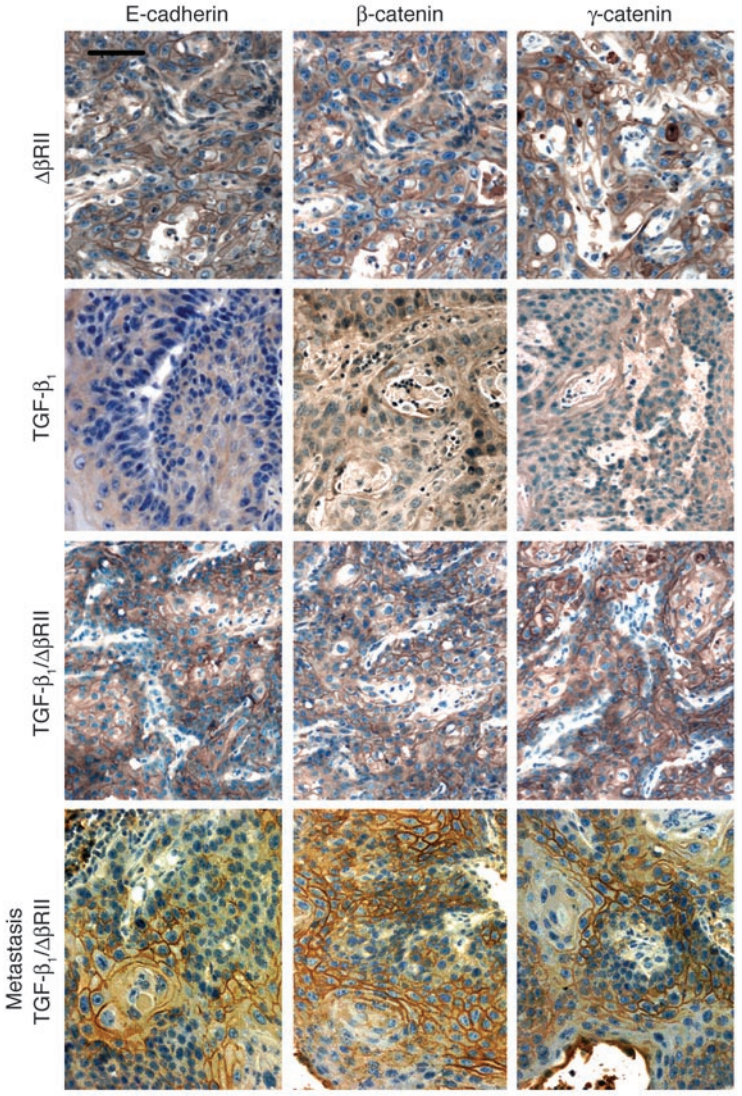

Figure 6
Immunohistochemical staining for E-cadherin and β- and γ-catenins in primary SCCs from ΔβRII-, TGF-β_1–, and TGF-β_1/ΔβRII–transgenic mice 25 weeks after DMBA initiation and in a lymph node metastasis from TGF-β_1/ΔβRII–transgenic SCCs. Note that all ΔβRII- and TGF-β_1/ΔβRII–transgenic SCCs and TGF-β_1/ΔβRII metastatic cells demonstrated staining for membrane-associated E-cadherin and β- and γ-catenins. Lung metastatic cells from TGF-β_1/ΔβRII–transgenic SCCs revealed a similar staining pattern (data not shown). However, these molecules appeared in the cytoplasm of cells in TGF-β_1–transgenic SCCs. Scale bar: 40 μm for all panels.

levels among TGF-β_1–, ΔβRII-, and TGF-β_1/ΔβRII–transgenic SCCs (about 5-fold higher than in control SCCs; Figure 7C). In control tumors, VEGFR1 expression was too low to be detected by RNase protection assay (RPA) (Figure 7C). In contrast, ΔβRII-transgenic SCCs exhibited a detectable level of VEGFR1 (Figure 7C). VEGFR1 expression levels in TGF-β_1– and TGF-β_1/ΔβRII–transgenic SCCs ranged from 2- to 5-fold higher than those in ΔβRII-transgenic SCCs (Figure 7C). We then examined SCCs at 25 weeks after DMBA initiation for expression levels of MMP-2 and MMP-9, both of which degrade the basement membrane (27) and also induce angiogenesis (28). Low levels of MMP-2 and MMP-9 expression were detected in control SCCs (Figure 7D). Both TGF-β_1– and ΔβRII-transgenic SCCs exhibited a 2- to 4-fold increase in expression of MMP-2 and MMP-9 compared with control SCCs (Figure 7D). The highest level of MMP-2 and MMP-9 expression was observed in TGF-β_1/ΔβRII–transgenic SCCs, which exhibited a 5-fold increase in MMP-2 expression and a 10-fold increase in MMP-9 expression compared with control SCCs (Figure 7D).

ΔβRII expression selectively blocked TGF-β1–induced expression of Jagged 1 and Hey1 but not Rho/Rac and MAPK signaling components. To understand how ΔβRII selectively blocked TGF-β_1–mediated EMT but not metastasis in skin carcinogenesis in vivo, we examined expression levels of signaling components of the Notch, Rho/Rac, and MAPK pathways that have been suggested to mediate TGF-β_1–mediated tumor invasion and EMT (29, 30). As shown in Figure 8A, expression of Jagged 1 (Jag1), a Notch ligand, and Hey1, a downstream target, was elevated 7- to 10-fold in the TGF-β_1–transgenic SCCs compared with control SCCs. However, expression of Jag1 and Hey1 in TGF-β_1/ΔβRII–transgenic SCCs was similar to that in control SCCs. With respect to expression of Rho/Rac signaling molecules, elevated expression of RhoA and Rac1 was observed in SCCs from ΔβRII-, TGF-β_1–, and TGF-β_1/ΔβRII–transgenic mice, ranging from 7- to 10-fold compared with their expression levels in control SCCs (Figure 8A). RhoC expression levels were similar among control and the various transgenic SCCs (data not shown). Among MAPK signaling components, mRNA levels of Erk1, Erk2, and JNK1 in SCCs from all 3 transgenic groups were increased approximately 5- to 20-fold compared with levels in control SCCs (Figure 8B). Expression levels of JNK2 were 2- to 3-fold higher in transgenic SCCs than in control SCCs (Figure 8B). Since activation of these molecules is independently regulated at the protein level by phosphorylation, we performed Western blot analysis for the total and phosphorylated forms of each of these molecules. Higher levels of total and phosphorylated Erk1/2 and JNK1/2 proteins were observed in the various transgenic SCCs compared with control SCCs (Figure 8C). Expression levels of another MAPK component, p38 kinase, were similar among transgenic and control SCCs at both the mRNA and protein levels (data not shown).

Discussion

In this study, we observed that TGF-β_1 was overexpressed and TGF-βRII was reduced in more than 50% of the human skin SCC samples we analyzed, and nearly 40% of the SCCs exhibited the combination of TGF-β_1 overexpression and TGF-βRII reduction. In our transgenic mouse models, we found that late-stage TGF-β_1 overexpression in chemically induced skin papillomas did not exert a tumor-suppressive effect. ΔβRII expression selectively blocked TGF-β_1–mediated EMT but cooperated with TGF-β_1 for tumor invasion.

Escaping TGF-β1–mediated growth inhibition is common in late-stage skin tumors. Our previous study demonstrated that TGF-β_1 transgene expression switches its function from a tumor suppressor to a tumor promoter after mid-stage skin carcinogenesis (6). Since TGF-β_1 expression was induced at a relatively early stage in that study, we could not rule out the possibility that long-term TGF-β_1 overexpression selects for TGF-β_1–resistant tumors that have a high

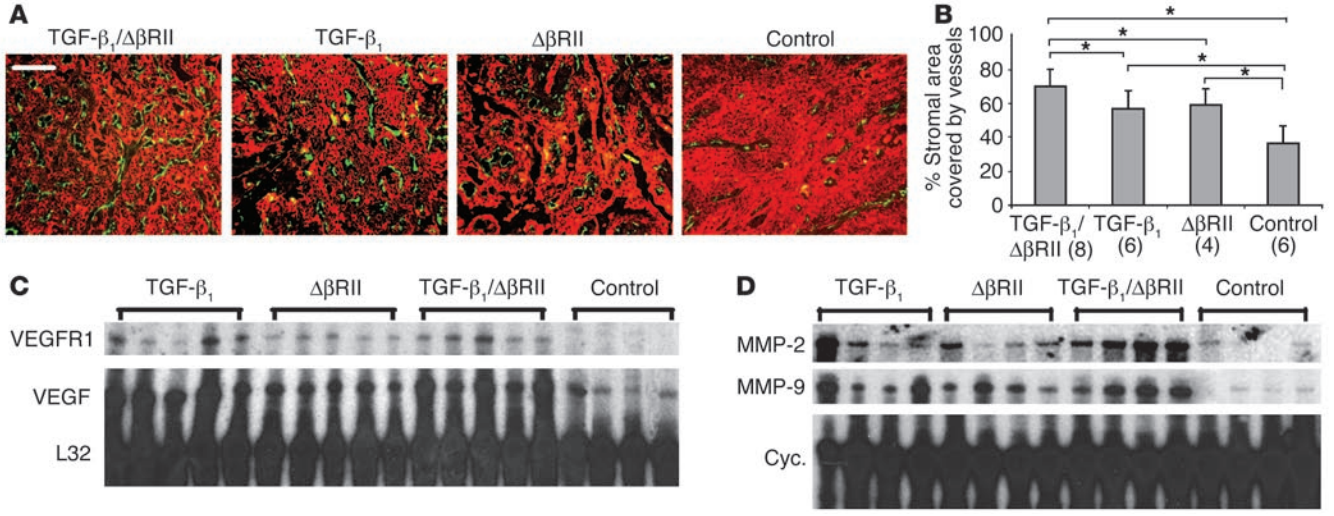

Figure 7

Angiogenesis and proteinase expression. (**A**) CD31 immunofluorescence. CD31 (green) highlights vessels. K14 (red) highlights the epithelial portion of tumors. Scale bar: 75 μm for all panels. (**B**) Percentage of the stromal area covered by vessels in TGF-β_1/ΔβRII–, TGF-β_1–, and ΔβRII-transgenic and control SCCs. The numbers in parentheses represents the number of tumors examined from each group. *$P < 0.05$. (**C** and **D**) Expression levels of VEGFR1 and VEGF (**C**) and MMP-2 and MMP-9 (**D**) detected by RPA in SCCs from TGF-β_1–, ΔβRII-, and TGF-β_1/ΔβRII–transgenic and control mice 25 weeks after DMBA initiation. L32 (**C**) or cyclophilin (Cyc.; **D**) was used to normalize the amount of RNA loaded in each lane.

malignant potential. To address this issue in the present study, we induced TGF-β_1 transgene expression after a full course of TPA promotion and performed BrdU labeling shortly after TGF-β_1 transgene induction in late-stage papillomas. We found that these papillomas were resistant to TGF-β_1–mediated growth inhibition. Loss of TGF-β_1–mediated growth arrest is apparently not due to spontaneous loss of TGF-β signaling, since increased nuclear pSmad2 protein was observed in TGF-β_1–transgenic papillomas. This contrasts with our previous observation that TGF-β_1 transgene expression accelerates the loss of its signaling components during skin chemical carcinogenesis (6). Thus, a relatively long term of TGF-β_1 overexpression is required for downregulation of TGF-β_1 signaling components, and the resistance to TGF-β_1–mediated growth inhibition in late-stage papillomas observed in this study might be attributable to the accumulation of more genetic insults than in the earlier-stage papillomas, which can override TGF-β_1–mediated growth arrest.

TGF-β_1–mediated EMT in vivo requires functional TGF-βRII. In vitro experiments using ΔβRII cell lines (8, 31), or xenografted cells transfected with ΔβRII (32) demonstrated that ΔβRII prevents TGF-β1–mediated EMT. Consistent with these reports, our results showed that TGF-β_1–mediated SPCC formation requires functional TGF-βRII in tumor epithelia during skin carcinogenesis, which indicates that the role of TGF-βRII in TGF-β_1–mediated EMT cannot be compensated for in vivo by other mechanisms. It has been suggested that TGF-β_1–mediated downregulation of E-cadherin, either at the transcriptional level (33, 34) or via disassembly of membrane-associated E-cadherin (35, 36), plays an important role in EMT. In cultured keratinocytes, TGF-β_1 induces the disassembly of E-cadherin via complex signal transduction pathways, including the Notch, MAPK, and Rho/Rac pathways (29, 37). In the present study, we found that TGF-β_1–transgenic SCCs exhibited either increased expression levels or activation of components of the above-mentioned signaling pathways. However, the blockade of EMT by ΔβRII was only correlated with reversed expression levels of Jag1 and Hey1 in TGF-β_1/ΔβRII–transgenic tumors, which suggests that changes in the other molecules may be functionally redundant for TGF-β_1–mediated EMT. A recent study has shown that expression of Hey1 is not only activated by Notch signaling, but can also be activated directly by TGF-β_1 in a Smad-dependent manner (37). Our current study shows that TGF-β_1–transgenic SCCs exhibited a very low level of pSmad2. This result is consistent with our previous observation that TGF-β_1 induces loss of membrane-associated E-cadherin when tumors begin to lose Smads (6). However, one report shows that Smad2 is required for TGF-β_1–mediated EMT in cultured SCC cells (22). It is possible that a very low level of pSmad2 in SCCs is sufficient for inducing expression of Jag1 and Hey1. Alternatively, since TGF-β_1 transgene expression was able to induce Jag1 and Hey1 expression before pSmad2 was lost (data not shown), it is possible that once Jag1 and Hey1 levels were elevated by Smads, they were maintained at a high level via their own positive feedback loop (37, 38) and thus no longer required Smads. Since blockade of TGF-β_1–induced Jag1 and Hey1 correlated with abrogation of TGF-β_1–mediated loss of membrane-associated E-cadherin/catenin and SPCC formation, our data suggest that these 2 molecules play an indispensable role in TGF-β_1–mediated EMT during skin carcinogenesis in vivo.

TGF-β_1 overexpression and loss of functional TGF-βRII cooperate for tumor invasion. Although ΔβRII expression blocked TGF-β_1–mediated EMT, malignant conversion and metastasis still occurred at the highest rate in TGF-β_1/ΔβRII–transgenic tumors. Furthermore, many metastatic cancer cells from TGF-β_1/ΔβRII– or ΔβRII-transgenic SCCs still retain membrane-associated E-cadherin/catenin. These results suggest that even though loss of membrane-associated E-cadherin is required for EMT, this event is dispensable for tumor metastasis. In addition to being involved in EMT, the Rho/Rac pathway is documented as a metastasis-associated pathway (39), and elevated levels of Erk and JNK have been observed in invasive skin SCCs (40, 41). Specifically, both the RhoA/Rac and the MAPK pathways have been documented to significantly affect cell motility (42, 43). Once cancer cells have

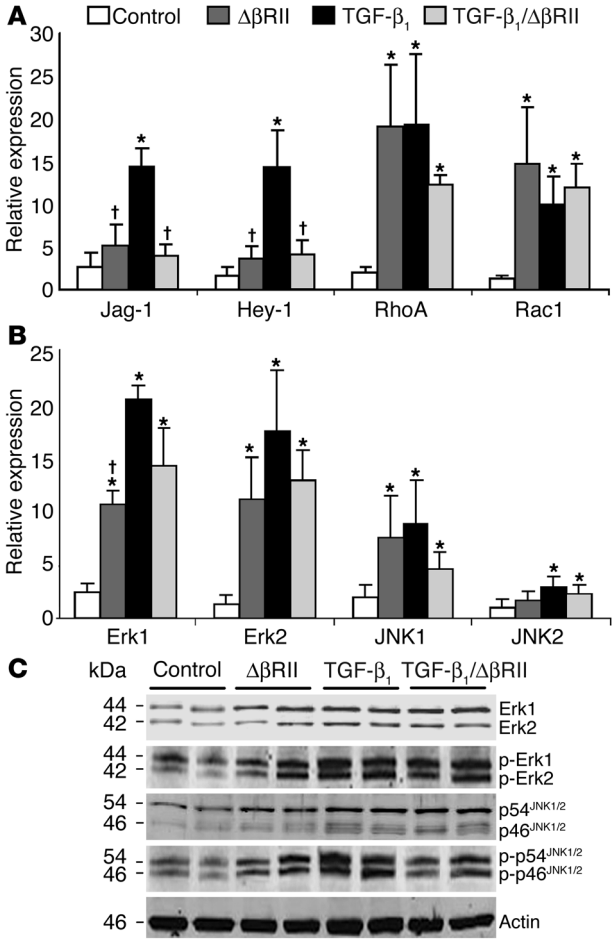

Figure 8
Analysis of Notch, Rho/Rac, and MAPK signaling components in SCC samples with different genotypes. Data were averaged from 5 SCCs from each group. One control SCC with the lowest expression level of individual molecules was assigned the value of 1 arbitrary unit as determined by quantitative RT-PCR in **A** and **B**. *$P < 0.05$ compared with control SCCs; †$P < 0.05$ compared with TGF-β_1–transgenic SCCs. (**C**) Western blot analysis of MAPK components. A pair of samples from each group is presented. Four to six samples in each group were examined and exhibited patterns similar to the representative samples shown here. p-Erk1, phosphorylated Erk1.

the ability to move out of the primary lesion, local proteinases and angiogenesis play crucial roles in distant metastasis formation. To this end, both the RhoA/Rac and the MAPK pathways have been documented to induce MMP expression and angiogenesis (42–44). Our data show that ΔβRII expression also upregulated the levels of RhoA, Erk, and JNK. This result may reflect 1 of the following 2 possibilities. First, the current level of ΔβRII expression preferentially blocked Smad signaling but could not completely abrogate upregulation of RhoA, Rac1, Erk, and JNK. Therefore, increased endogenous TGF-β_1 in ΔβRII-transgenic tumors or TGF-β_1 transgene expression in TGF-β_1/ΔβRII–transgenic tumors could upregulate these molecules in tumor cells via residual TGF-βRII signaling. Alternatively, levels of RhoA, Rac1, Erk, and JNK in ΔβRII- or TGF-β_1/ΔβRII–transgenic tumors may be elevated as a result of a secondary effect of ΔβRII expression, as tumors with ΔβRII transgene expression developed earlier than did TGF-β_1–transgenic tumors and thus presumably accumulated more genetic insults than TGF-β_1–transgenic tumors at the same time point. It is hopeful that future studies using an approach that completely ablates TGF-βRII in keratinocytes will further clarify this issue. If the first possibility proves to be true, ablation of TGF-βRII in keratinocytes will block both EMT and metastasis. Therefore, tumors with partial and complete loss of TGF-βRII (e.g., via mutation or promoter methylation vs. gene deletion) will have a different outcome and prognosis. However, if the second possibility proves to be true, ablation of TGF-βRII in keratinocytes will still uncouple TGF-β_1–mediated EMT and metastasis.

Since angiogenesis and expression levels of MMP-2 and MMP-9 were the greatest in TGF-β_1/ΔβRII–transgenic SCCs, ΔβRII apparently cooperated with TGF-β_1 overexpression in these processes. Obviously, ΔβRII expression in tumor epithelia cannot block the paracrine effect of TGF-β_1 on tumor stroma, an important factor in inducing MMPs and angiogenesis. However, this cooperation cannot be simply explained by TGF-β_1 levels in TGF-β_1/ΔβRII–transgenic tumors, since they were similar to those in TGF-β_1–transgenic tumors. It is likely that ΔβRII expression allows the accumulation of other oncogenic events, which synergistically interact with the paracrine effect of TGF-β_1 overexpression on the upregulation of MMPs and VEGF. These oncogenic events may have occurred at stages prior to the spontaneous loss of TGF-β_1–induced growth inhibition in wild-type tumors. Alternatively, the oncogenic events elicited by ΔβRII expression may also result from the blocking of other TGF-β_1–mediated tumor-suppressive effects that are independent of TGF-β_1–mediated growth arrest (1). Although in either case, the tumor suppressive effects of TGF-β_1 should counteract its paracrine effect on tumor invasion, these effects appeared to be abrogated in TGF-β_1/ΔβRII–transgenic tumors.

In summary, our study revealed that TGF-β_1–mediated tumor invasion and EMT can be uncoupled. Figure 9 depicts the potential underlying mechanisms of these 2 distinct functions of TGF-β_1. TGF-β_1–mediated EMT relies on functional TGF-βRII to deregu-

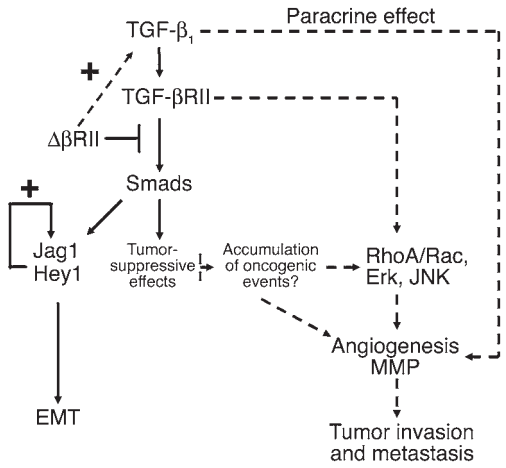

Figure 9
Schematic depicting the potential mechanisms of uncoupling TGF-β_1–mediated EMT and tumor invasion by ΔβRII expression. The dotted lines indicate potential mechanisms of the cooperative effects between TGF-β_1 overexpression and ΔβRII expression on tumor invasion and metastasis.

late epithelial adhesion molecules, depending, at least in part, on the activation of Jag1 and Hey1. Jag1 and Hey1 are upregulated via a Smad-dependent pathway at early stages, and their expression levels are maintained via their own positive feedback loop once expression of Smads is lost. In contrast, TGF-β_1–mediated metastasis largely relies on proteinase activation and angiogenesis, which are mainly mediated by increased levels of RhoA/Rac, Erk, and JNK. ΔβRII expression either cannot completely block TGF-βRII–mediated activation of these pathways and therefore activates these pathways via increased endogenous TGF-β_1, or it leads to activation of these pathways via other oncogenic events accumulating in the absence of TGF-β_1–mediated growth arrest. In addition, the accumulated additional oncogenic events in TGF-β_1/ΔβRII–transgenic tumors due to blocking TGF-β_1–mediated tumor-suppressive effects in tumor epithelia cooperate with the paracrine effect of TGF-β_1 on tumor stroma to achieve tumor invasion and metastasis. Our results warrant future studies using both clinical samples and experimental models to further determine whether skin SCCs that have both increased TGF-β_1 and reduced TGF-βRII will have a poor prognosis.

Methods

Human skin cancer sample collection. We collected tissue samples between the years 2001 and 2004 from consenting patients under a protocol approved by the Institutional Review Board at the Oregon Health & Science University. Normal human skin from healthy volunteers was obtained via punch biopsy or cosmetic surgeries that removed the excess skin. Skin tumors were surgically removed. H&E-stained sections were prepared from all tissue samples and were reviewed by a dermatopathologist for diagnosis.

Immunohistochemical staining. Immunohistochemistry was performed on formalin-fixed tumor sections as previously described (11). Staining for TGF-β_1 and TGF-βRII was performed as previously described (45) using TGF-β_1 (R&D Systems) or TGF-βRII antibodies (Santa Cruz Biotechnology Inc.). Blocking peptides specific for each antibody were included as negative controls. Cell adhesion molecules in mouse tumor samples were stained as previously described (6), using antibodies specific for E-cadherin, β-catenin, and γ-catenin (BD Biosciences — Pharmingen). Staining of pSmad2 was performed using a pSmad2 antibody (Cell Signaling Technology). The immune complexes were detected by the avidin-biotin-peroxidase complex using Vectastain kits (Vector Laboratories) and visualized with diaminobenzidine. Sections were counterstained with hematoxylin. Protein levels detected by immunohistochemistry were visually evaluated. A double-blind evaluation was performed by 2 investigators using the methods described by Yang et al. (46) with modifications. Briefly, signal intensity was scored as 0 (no intensity), 1 (weak intensity), 2 (moderate), or 3 (strong). For each tissue section, the percentage of positive cells within each of the 4 intensity categories was estimated and multiplied by the corresponding intensity score. The 4 partial scores obtained in each section were added and expressed as a final score. The staining intensity in normal epidermis was determined to be 1 for TGF-β_1, 3 for TGF-βRII, and 0 for pSmad2. Therefore, a score of 1.5 or higher for TGF-β_1 was considered as increased staining; less than 2.5 for TGF-βRII as decreased staining; and above 0 for Smad2 as positive staining.

Transgenic mice. The generation of transgenic mice and the procedures used were approved by the Institutional Animal Care and Use Committee of the Oregon Health & Science University. All of the transgenic lines were generated in the ICR strain, and transgene expression was achieved using a *mouse loricrin* (*ML*) promoter, which targets transgene expression to the interfollicular epidermis and through all stages of skin carcinogenesis, including metastatic lesions (11). We generated TGF-β_1–transgenic mice by mating the *ML.GLVPc* transactivator line with the *tk.TGF-*β_1 target line, in which a modified *thymidine kinase* (*tk*) promoter precedes the *TGF-*β_1 transgene (23). *ML.GLVPc/tk.TGF-*β_1 bigenic mice were also crossbred to *ML.*Δβ*RII*-transgenic mice (24) to generate *ML.GLVPc/tk.TGF-*β_1*/ML.*Δβ*RII*–transgenic mice.

Skin chemical carcinogenesis and TGF-β_1 *transgene induction*. A chemical carcinogenesis protocol was applied to 8-week-old mice, as previously described (11). Briefly, 50 μg of DMBA was topically applied to the shaved back skin. One week after DMBA initiation, mice were topically treated with 5 μg TPA, once a week for 20 weeks. TGF-β_1 transgene expression was induced by topical application of a progesterone antagonist, RU486, to skin tumors of bigenic TGF-β_1– or TGF-β_1/ΔβRII–transgenic mice (Figure 2A). RU486 was given at a dose of 20 μg/mouse (dissolved in 100 μl of 70% ethanol), 3 times per week, beginning at 20 weeks after DMBA initiation. Control mice and ΔβRII-transgenic mice were also treated with RU486 or with ethanol.

Histological analysis. Tumors were fixed in 10% neutral buffered formalin at 4°C overnight, embedded in paraffin, sectioned to 6 μm, and stained with H&E. Tumor types were histologically determined following the criteria described by Aldaz et al. (47).

Immunofluorescence staining for BrdU labeling and CD31. Tumor-bearing mice at 20 weeks after DMBA initiation were treated with RU486 (20 μg, 3 times/week). Eleven hours after the third RU486 treatment, BrdU (125 mg/kg in 0.9% NaCl) was injected (i.p.) into these mice. Papillomas and adjacent skin from TGF-β_1–transgenic and control mice were dissected 2 hours after the injection, fixed, and processed as previously described (48). Sections were incubated with an FITC-conjugated monoclonal antibody to BrdU (BD Biosciences) and a guinea-pig antiserum to mouse keratin 14 (K14), which reacts with the epithelial component of papillomas. K14 was visualized using Alexa 594–conjugated anti-guinea-pig IgG (Invitrogen Corp.). Consecutive fields of BrdU-labeled cells were counted throughout the entire tissue section. Five papillomas and adjacent skins were analyzed in each group. The labeling index was expressed as the mean number of BrdU-positive cells/mm basement membrane ± SD. Immunofluorescence staining of CD31 and quantitation of blood vessels were performed as previously described (11).

RNA analyses. Skin and tumor RNA was isolated with RNAzol B (Tel-Test Inc.) as previously described (24) and purified using a QIAGEN RNeasy kit (QIAGEN). Quantitative RT-PCR was performed as previously described (49). TaqMan Assays-on-Demand probes (Applied Biosystems) were used to detect transcripts of mouse Jag1, Hey1, RhoA, RhoC, Rac1, Erk1, Erk2, JNK1, JNK2, and p38. An 18S RNA probe was used as an internal control, and the data (cycle of threshold [C_T] values) were analyzed using the ΔC_T method. The results were averaged from 5 mice of each group, and 1 control sample with the lowest expression level of each individual molecule was assigned the value of 1 arbitrary unit. We used RT-PCR to detect TGF-β_1 transgene expression in transgenic tumor samples, using primers specific for porcine TGF-β_1 (23). We performed RPAs using the RPA II kit (Ambion) and ^{32}P-labeled riboprobes. The MMP-2 and MMP-9 probes were made as previously described (6). The VEGF and VEGFR1 probes were from the mouse angiogenesis-1 multiprobe set from BD Biosciences — Pharmingen. A riboprobe for L32 or cyclophilin was used as a loading control. The intensity of bands representing protected transcripts was determined by densitometric scanning of x-ray films.

Protein analyses. Skin and tumor proteins were extracted as previously described (49). The amount of TGF-β_1 protein was measured by TGF-β_1–specific ELISA as previously described (49). We performed Western blot analysis as previously described (49) using antibodies specific for total and phosphorylated Erk, JNK, and p38 (Cell Signaling Technology).

Statistical analysis. Significant differences between 2 data groups were analyzed using the Student's *t* test with exception of the data presented in Table 1 and Table 3, which were analyzed by the χ^2 test.

Acknowledgments

This work was supported by NIH grants CA79998 and CA87849 (to X.-J. Wang). We thank the Molecular Profiling Resource of the Departments of Dermatology and Otolaryngology, Oregon Health & Science University for providing skin SCC samples.

Received for publication January 5, 2005, and accepted in revised form April 19, 2005.

Address correspondence to: Xiao-Jing Wang, Departments of Otolaryngology, Dermatology, and Cell and Developmental Biology, Oregon Health & Science University, PVMC Building 103-F221, R&D46, 3710 SW US Veterans Hospital Road, Portland, Oregon 97239, USA. Phone: (503) 220-8262 ext. 54273; Fax: (503) 402-2817; E-mail: wangxiao@ohsu.edu.

1. Roberts, A.B., and Wakefield, L.M. 2003. The two faces of transforming growth factor beta in carcinogenesis. *Proc. Natl. Acad. Sci. U. S. A.* **100**:8621–8623.
2. Gold, L.I. 1999. The role for transforming growth factor-beta (TGF-beta) in human cancer. *Crit. Rev. Oncog.* **10**:303–360.
3. Reiss, M. 1999. TGF-beta and cancer. *Microbes Infect.* **1**:1327–1347.
4. Lu, S.L., et al. 2004. Overexpression of transforming growth factor beta1 in head and neck epithelia results in inflammation, angiogenesis, and epithelial hyperproliferation. *Cancer Res.* **64**:4405–4410.
5. Wang, X.J. 2001. Role of TGFbeta signaling in skin carcinogenesis. *Microsc. Res. Tech.* **52**:420–429.
6. Weeks, B.H., He, W., Olson, K.L., and Wang, X.J. 2001. Inducible expression of transforming growth factor beta1 in papillomas causes rapid metastasis. *Cancer Res.* **61**:7435–7443.
7. Derynck, R., and Zhang, Y.E. 2003. Smad-dependent and Smad-independent pathways in TGF-beta family signalling. *Nature.* **425**:577–584.
8. Oft, M., Heider, K.H., and Beug, H. 1998. TGFbeta signaling is necessary for carcinoma cell invasiveness and metastasis. *Curr. Biol.* **8**:1243–1252.
9. Yin, J.J., et al. 1999. TGF-beta signaling blockade inhibits PTHrP secretion by breast cancer cells and bone metastases development. *J. Clin. Invest.* **103**:197–206.
10. Tang, B., et al. 2003. TGF-beta switches from tumor suppressor to prometastatic factor in a model of breast cancer progression. *J. Clin. Invest.* **112**:1116–1124. doi:10.1172/JCI200318899.
11. Go, C., Li, P., and Wang, X.J. 1999. Blocking transforming growth factor beta signaling in transgenic epidermis accelerates chemical carcinogenesis: a mechanism associated with increased angiogenesis. *Cancer Res.* **59**:2861–2868.
12. Tu, W.H., et al. 2003. The loss of TGF-beta signaling promotes prostate cancer metastasis. *Neoplasia*. **5**:267–277.
13. Fukai, Y., et al. 2003. Reduced expression of transforming growth factor-beta receptors is an unfavorable prognostic factor in human esophageal squamous cell carcinoma. *Int. J. Cancer.* **104**:161–166.
14. Miyajima, A., Asano, T., Seta, K., Kakoi, N., and Hayakawa, M. 2003. Loss of expression of transforming growth factor-beta receptor as a prognostic factor in patients with renal cell carcinoma. *Urology.* **61**:1072–1077.
15. Watanabe, T., et al. 2001. Molecular predictors of survival after adjuvant chemotherapy for colon cancer. *N. Engl. J. Med.* **344**:1196–1206.
16. Tateishi, M., et al. 2000. The progression of invasiveness regarding the role of transforming growth factor beta receptor type II in gastric cancer. *Eur. J. Surg. Oncol.* **26**:377–380.
17. Gold, L.I., Jussila, T., Fusenig, N.E., and Stenback, F. 2000. TGF-beta isoforms are differentially expressed in increasing malignant grades of HaCaT keratinocytes, suggesting separate roles in skin carcinogenesis. *J. Pathol.* **190**:579–588.
18. Huntley, S.P., et al. 2004. Attenuated type II TGF-beta receptor signalling in human malignant oral keratinocytes induces a less differentiated and more aggressive phenotype that is associated with metastatic dissemination. *Int. J. Cancer.* **110**:170–176.
19. DiGiovanni, J. 1992. Multistage carcinogenesis in mouse skin. *Pharmacol. Ther.* **54**:63–128.
20. Cui, W., et al. 1996. TGFbeta1 inhibits the formation of benign skin tumors, but enhances progression to invasive spindle carcinomas in transgenic mice. *Cell.* **86**:531–542.
21. Miettinen, P.J., Ebner, R., Lopez, A.R., and Derynck, R. 1994. TGF-beta induced transdifferentiation of mammary epithelial cells to mesenchymal cells: involvement of type I receptors. *J. Cell Biol.* **127**:2021–2036.
22. Oft, M., Akhurst, R.J., and Balmain, A. 2002. Metastasis is driven by sequential elevation of H-ras and Smad2 levels. *Nat. Cell Biol.* **4**:487–494.
23. Wang, X.J., Liefer, K.M., Tsai, S., O'Malley, B.W., and Roop, D.R. 1999. Development of gene-switch transgenic mice that inducibly express transforming growth factor beta1 in the epidermis. *Proc. Natl. Acad. Sci. U. S. A.* **96**:8483–8488.
24. Wang, X.J., et al. 1997. Expression of a dominant-negative type II transforming growth factor beta (TGF-beta) receptor in the epidermis of transgenic mice blocks TGF-beta-mediated growth inhibition. *Proc. Natl. Acad. Sci. U. S. A.* **94**:2386–2391.
25. Vegeto, E., et al. 1992. The mechanism of RU486 antagonism is dependent on the conformation of the carboxy-terminal tail of the human progesterone receptor. *Cell.* **69**:703–713.
26. He, W., Cao, T., Smith, D.A., Myers, T.E., and Wang, X.J. 2001. Smads mediate signaling of the TGFbeta superfamily in normal keratinocytes but are lost during skin chemical carcinogenesis. *Oncogene.* **20**:471–483.
27. MacDougall, J.R., and Matrisian, L.M. 1995. Contributions of tumor and stromal matrix metalloproteinases to tumor progression, invasion and metastasis. *Cancer Metastasis Rev.* **14**:351–362.
28. Bergers, G., et al. 2000. Matrix metalloproteinase-9 triggers the angiogenic switch during carcinogenesis. *Nat. Cell Biol.* **2**:737–744.
29. Zavadil, J., et al. 2001. Genetic programs of epithelial cell plasticity directed by transforming growth factor-beta. *Proc. Natl. Acad. Sci. U. S. A.* **98**:6686–6691.
30. Siegel, P.M., Shu, W., Cardiff, R.D., Muller, W.J., and Massague, J. 2003. Transforming growth factor beta signaling impairs Neu-induced mammary tumorigenesis while promoting pulmonary metastasis. *Proc. Natl. Acad. Sci. U. S. A.* **100**:8430–8435.
31. Bhowmick, N.A., Zent, R., Ghiassi, M., McDonnell, M., and Moses, H.L. 2001. Integrin beta 1 signaling is necessary for transforming growth factor-beta activation of p38MAPK and epithelial plasticity. *J. Biol. Chem.* **276**:46707–46713.
32. Portella, G., et al. 1998. Transforming growth factor beta is essential for spindle cell conversion of mouse skin carcinoma in vivo: implications for tumor invasion. *Cell Growth Differ.* **9**:393–404.
33. Comijn, J., et al. 2001. The two-handed E box binding zinc finger protein SIP1 downregulates E-cadherin and induces invasion. *Mol. Cell.* **7**:1267–1278.
34. Peinado, H., Quintanilla, M., and Cano, A. 2003. Transforming growth factor beta-1 induces snail transcription factor in epithelial cell lines: mechanisms for epithelial mesenchymal transitions. *J. Biol. Chem.* **278**:21113–21123.
35. Bakin, A.V., Tomlinson, A.K., Bhowmick, N.A., Moses, H.L., and Arteaga, C.L. 2000. Phosphatidylinositol 3-kinase function is required for transforming growth factor beta-mediated epithelial to mesenchymal transition and cell migration. *J. Biol. Chem.* **275**:36803–36810.
36. Bhowmick, N.A., et al. 2001. Transforming growth factor-beta1 mediates epithelial to mesenchymal transdifferentiation through a RhoA-dependent mechanism. *Mol. Biol. Cell.* **12**:27–36.
37. Zavadil, J., Cermak, L., Soto-Nieves, N., and Bottinger, E.P. 2004. Integration of TGF-beta/Smad and Jagged1/Notch signalling in epithelial-to-mesenchymal transition. *EMBO J.* **23**:1155–1165.
38. Ross, D.A., and Kadesch, T. 2004. Consequences of Notch-mediated induction of Jagged1. *Exp. Cell Res.* **296**:173–182.
39. Ridley, A.J. 2001. Rho GTPases and cell migration. *J. Cell Sci.* **114**:2713–2722.
40. Dajee, M., et al. 2003. NF-kappaB blockade and oncogenic Ras trigger invasive human epidermal neoplasia. *Nature.* **421**:639–643.
41. Zhang, J.Y., Tao, S., Adams, A., and Khavari, P.A. 2004. JNK activation and oncogenic Ras trigger invasive human epidermal neoplasia [abstract]. *J. Invest. Dermatol.* **122**:590.
42. Sahai, E., and Marshall, C.J. 2002. RHO-GTPases and cancer. *Nat. Rev. Cancer.* **2**:133–142.
43. Reddy, K.B., Nabha, S.M., and Atanaskova, N. 2003. Role of MAP kinase in tumor progression and invasion. *Cancer Metastasis Rev.* **22**:395–403.
44. Bachelor, M.A., and Bowden, G.T. 2004. Ultraviolet A-induced modulation of Bcl-XL by p38 MAPK in human keratinocytes: post-transcriptional regulation through the 3′-untranslated region. *J. Biol. Chem.* **279**:42658–42668.
45. He, W., et al. 2002. Overexpression of Smad7 results in severe pathological alterations in multiple epithelial tissues. *EMBO J.* **21**:2580–2590.
46. Yang, X., Groshen, S., Formenti, S.C., Davidson, N.E., and Press, M.F. 2003. P7 antigen expression in human breast cancer. *Clin. Cancer Res.* **9**:201–206.
47. Aldaz, C.M., Conti, C.J., Klein-Szanto, A.J., and Slaga, T.J. 1987. Progressive dysplasia and aneuploidy are hallmarks of mouse skin papillomas: relevance to malignancy. *Proc. Natl. Acad. Sci. U. S. A.* **84**:2029–2032.
48. Go, C., et al. 2000. Aberrant cell cycle progression contributes to the early-stage accelerated carcinogenesis in transgenic epidermis expressing the dominant negative TGFbetaRII. *Oncogene.* **19**:3623–3631.
49. Li, A.G., Wang, D., Feng, X.H., and Wang, X.J. 2004. Latent TGFbeta1 overexpression in keratinocytes results in a severe psoriasis-like skin disorder. *EMBO J.* **23**:1770–1781.